Figures and figure supplements

Blood flow guides sequential support of neutrophil arrest and diapedesis by PILR-β 1 and PILR-α

Yu-Tung Li *et al*

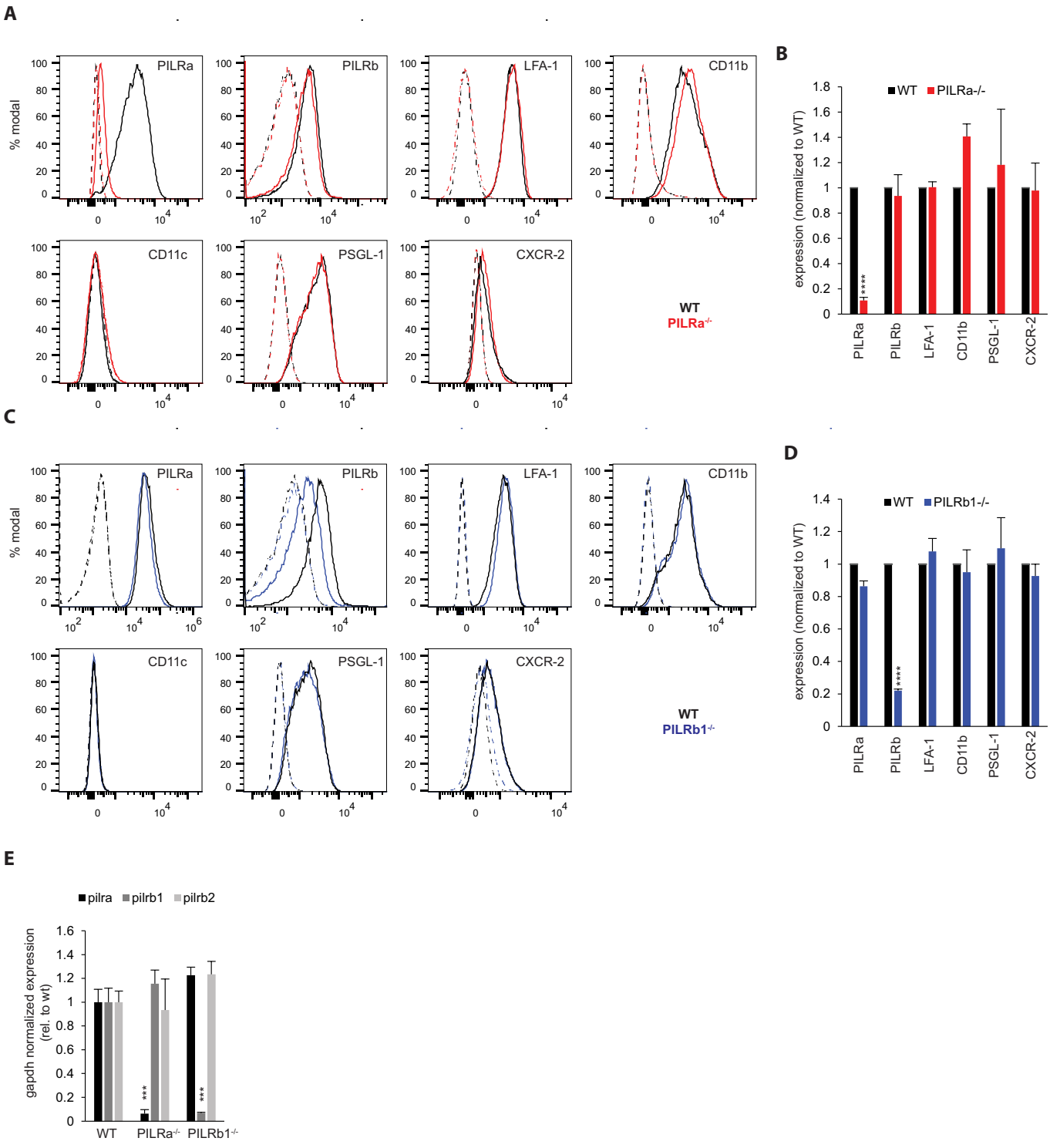

Figure 1. Characterization of PILR-$\alpha^{-/-}$ and PILR-$\beta1^{-/-}$neutrophils for surface expression of molecules involved in extravasation. Ly6G^{+} bone marrow neutrophils from WT, PILR-$\alpha^{-/-}$ or PILR$\beta1^{-/-}$ mice were analyzed for indicated antigens by FACS. Representative histograms of at least three independent experiments are shown in (**A**) for PILR-$\alpha^{-/-}$ and (**C**) for PILR-$\beta1^{-/-}$ mice, with expression levels quantified in (**B**) and (**D**), respectively. Solid tracks, specific staining; dotted tracks, isotype control. Groups were compared by 2-tailed t-test. (**E**) qRT-PCR analysis of RNA extracted from peripheral blood of WT

Figure 1 continued on next page

Figure 1 continued

(n = 9) or PILR-$\alpha^{-/-}$ (n = 5) or PILR-$\beta1^{-/-}$ (n = 7) mice for the indicated genes. Groups were analyzed by 1-way ANOVA followed by Holm-Sidak method for multiple comparisons. Error bars, SEM. ****p<0.001.

DOI: https://doi.org/10.7554/eLife.47642.002

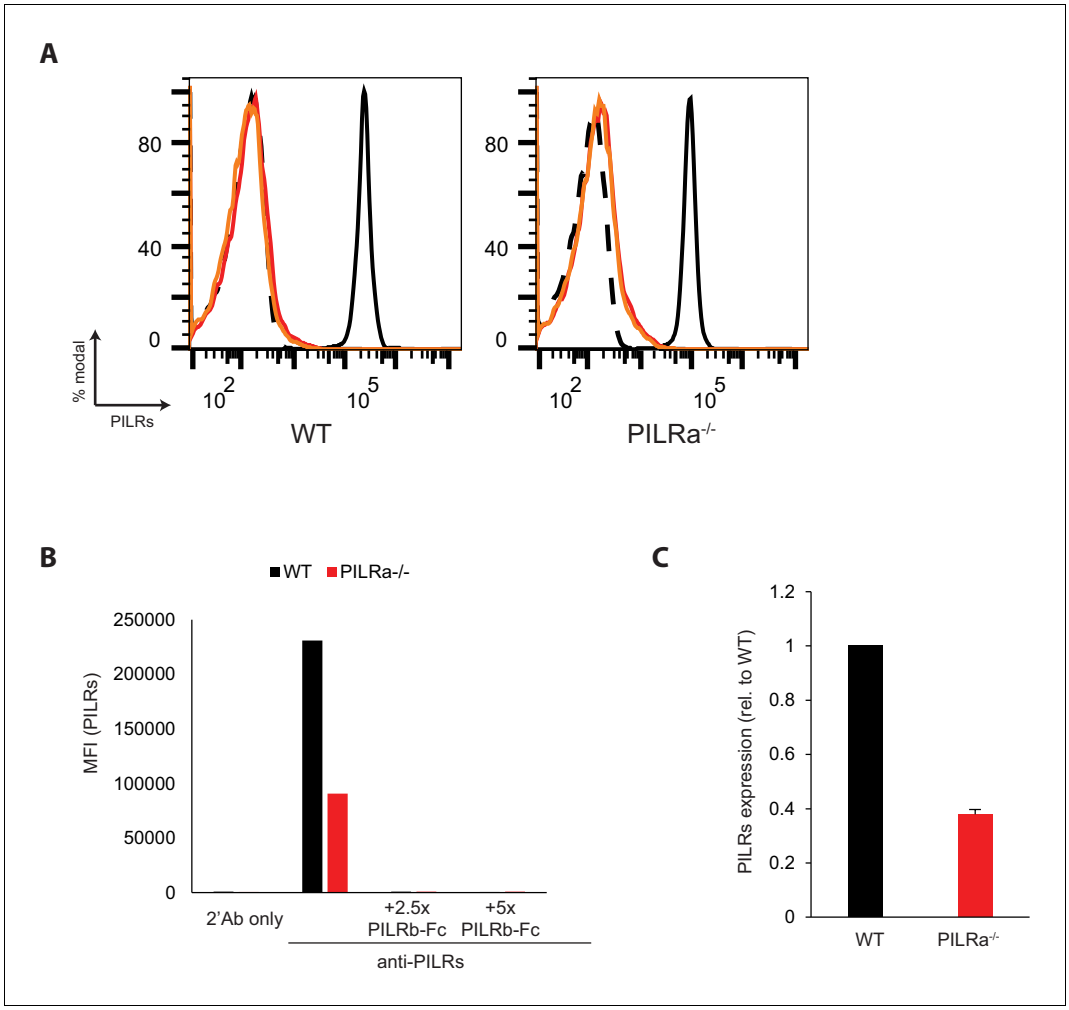

Figure 1—figure supplement 1. Quantification of PILR subtypes neutrophils. (**A**) Ly6G$^+$ WT and PILR-$\alpha^{-/-}$ bone marrow cells were stained with a primary antibody recognizing both PILR-α and PILR-β in the absence (black) or presence of 2.5-fold (red) or 5-fold (orange) excess of blocking PILR-β-Fc. Dotted black line: secondary antibody only, solid black line: without blocking PILR-β-Fc. (**B**) MFI quantification of PILRs signals in (**A**). (**C**) Quantification of PILRs signal on WT and PILR-$\alpha^{-/-}$ Ly6G$^+$ cells from two experiments.

DOI: https://doi.org/10.7554/eLife.47642.003

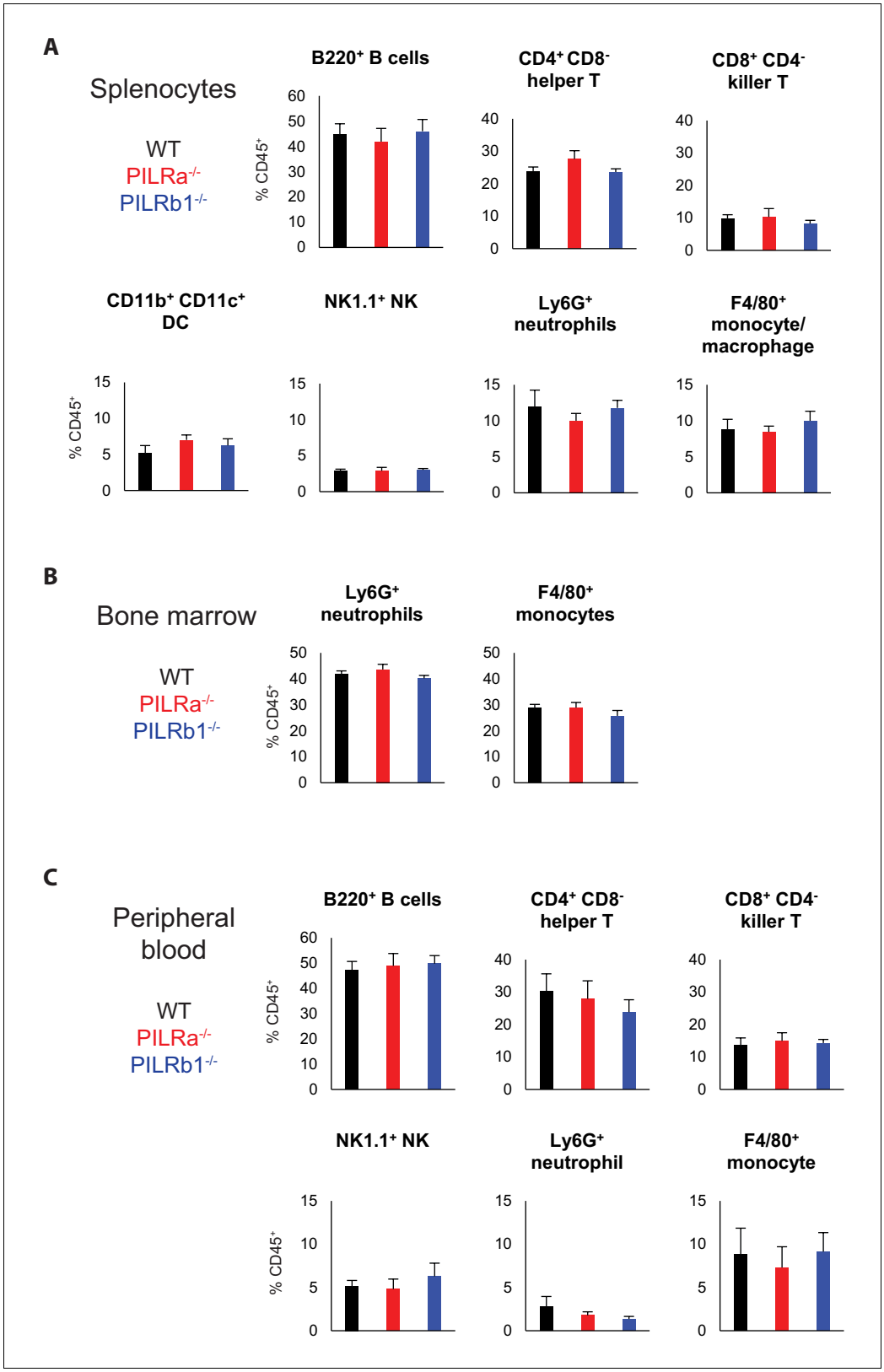

Figure 1—figure supplement 2. Characterization of immune subsets in PILR-$\alpha^{-/-}$ and PILR-$\beta1^{-/-}$mice. WT (black), PILR-$\alpha^{-/-}$ (red) and PILR-b$1^{-/-}$ (blue) CD45^{+} leukocytes from spleen (**A**), bone marrow (**B**) or peripheral blood (**C**)

Figure 1—figure supplement 2 continued on next page

Figure 1—figure supplement 2 continued

were stained by antibodies against the indicated antigens and analyzed by flow cytometry. Results are from at least three mice per genotype.

DOI: https://doi.org/10.7554/eLife.47642.005

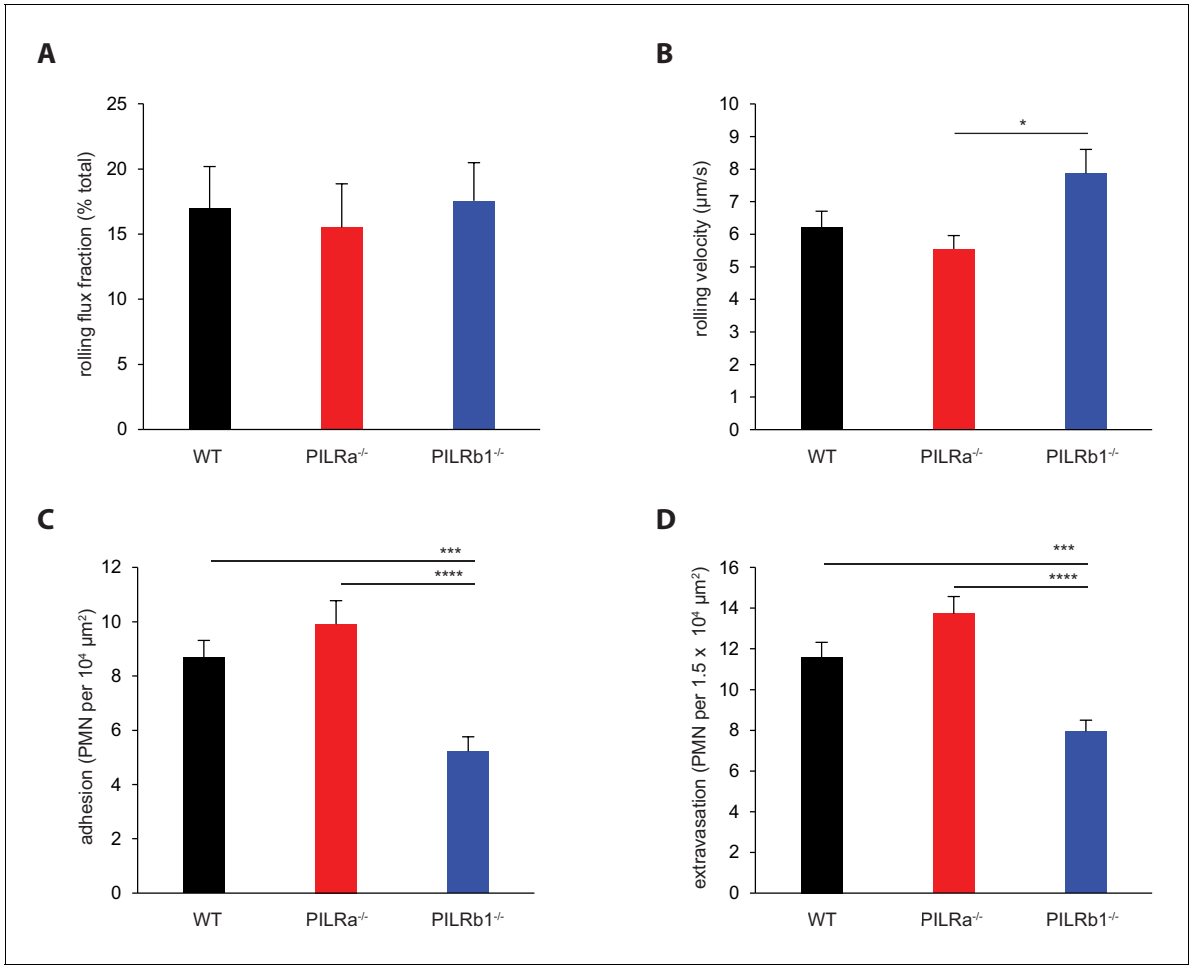

Figure 2. Impact of PILRs on neutrophil extravasation in the inflamed cremaster. WT, PILR-$\alpha^{-/-}$ and PILR-$\beta1^{-/-}$ mice were stimulated with intrascrotal TNF-α for 2 hr. Cremaster muscles were exposed and examined for neutrophil extravasation by intravital microscopy (IVM) for (**A**) rolling flux fraction, (**B**) rolling velocity, (**C**) adherent leukocytes, and (**D**) extravasated leukocytes. WT: n = 40 vessels from eight mice; PILR-$\alpha^{-/-}$: n = 37 vessels from seven mice; PILR-$\beta1^{-/-}$: n = 35 vessels from seven mice. For (**B**), 117 cells (WT), 111 cells (PILR-$\alpha^{-/-}$) and 105 cells (PILR-$\beta1^{-/-}$) from the indicated number of vessels were quantified. Groups were analyzed by 1-way ANOVA followed by Tukey's multiple comparisons. Error bars, SEM. *p<0.05, ***p<.005, ****p<0.001. Hemodynamic parameters are given in ***Table 1***.

DOI: https://doi.org/10.7554/eLife.47642.012

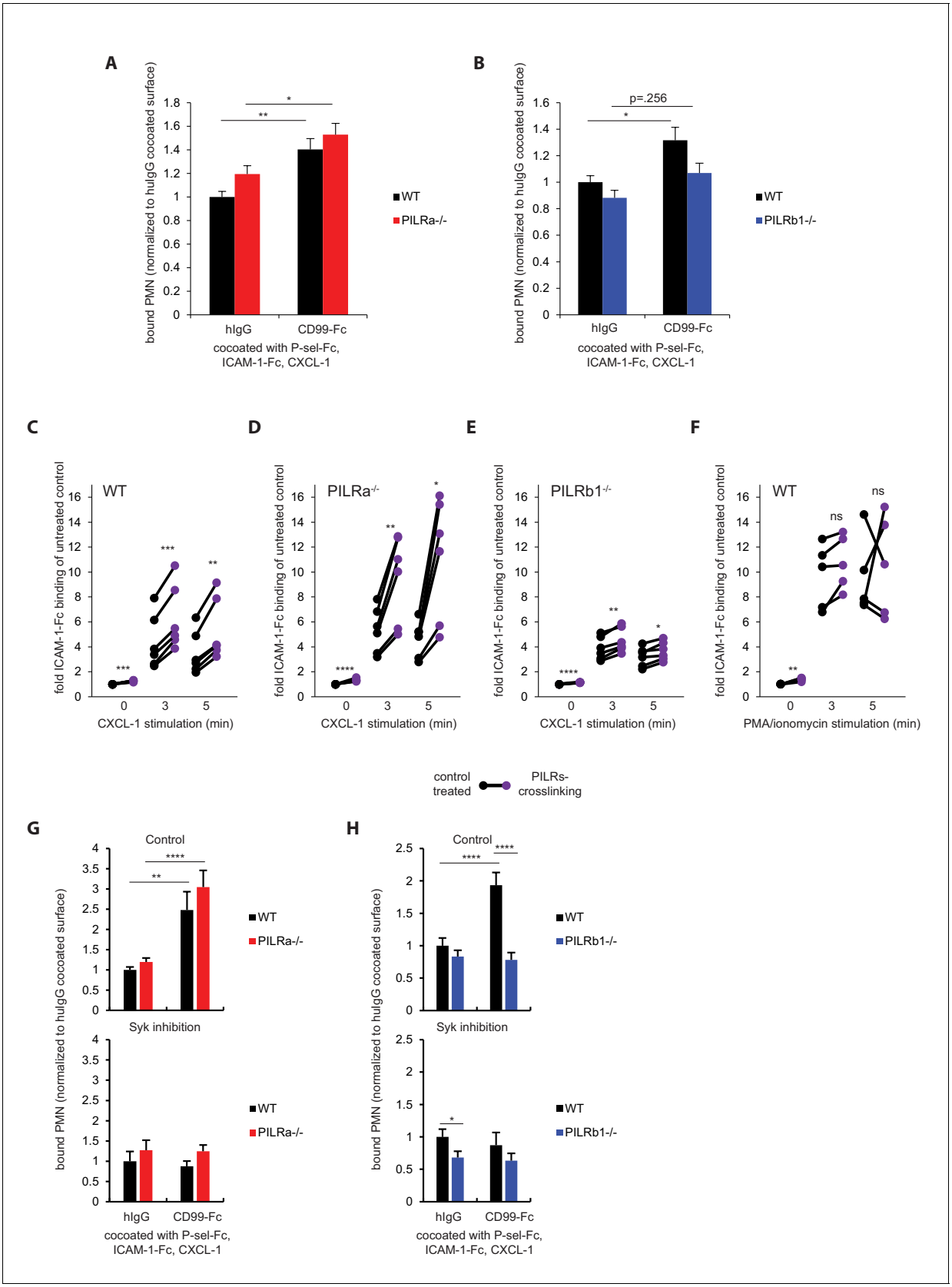

Figure 3. PILR-β1 is required for CD99-stimulated neutrophil adhesion on ICAM-1-Fc in vitro. Flow chamber surfaces were coated with P-selectin-Fc, ICAM-1-Fc and CXCL-1, and co-coated with either CD99-Fc or human IgG1 control (hIgG). PILR-$\alpha^{-/-}$ (**A**) or PILR-$\beta1^{-/-}$ (**B**) PMN were mixed with

Figure 3 continued on next page

Figure 3 continued

fluorescently labeled WT PMN in 1:1 ratio and passed over the surfaces at 5 dyn/cm^2 at 37°C for 5 min. Adherent PMNs were quantified for n = 45 fields from nine experiments each. (**C–E**) Bone marrow cells from WT (**C**), PILR-$\alpha^{-/-}$ (**D**) or PILR-$\beta1^{-/-}$ (**E**) mice were mixed with ICAM-1-Fc/PE-conjugated secondary antibody detection complex. Cell mixtures were pre-treated with non-crosslinking rabbit IgG or crosslinking polyclonal anti-PILRs in pair for 15 min, and then stimulated with 100 ng/ml CXCL-1 for 0 min (unstimulated), 3 and 5 min, followed by fixation and analysis for ICAM-1-Fc binding to Ly6G$^+$ cells by FACS. n = 6 paired samples per treatment per genotype. (**F**) Experiment described in (**C**) was repeated except for replacing the chemokine stimulation by 20 ng/ml PMA + 1 µg/ml ionomycin. n = 5 paired samples per treatment. (**G–H**) Experiments described in (**A–B**) were repeated in the presence of 1 µM Syk inhibitor PRT-060318 or vehicle control with PILR-$\alpha^{-/-}$ (**G**) or PILR-$\beta1^{-/-}$ (**H**) neutrophils. n = 26 fields each from two experiments (G, control) or 39 fields each from three experiments (G, inhibition) fields. n = 20 fields each from two experiments (H, control) or 30 fields each from three experiments (H, inhibition) fields. Groups were compared by 1-way ANOVA followed by Tukey's multiple comparisons in (**A, B, G, H**) or 2-tailed paired t-test in (**C–F**). Error bars, SEM. *p<0.05, **p<.005, ***p<0.0005, ****p<0.0001.

DOI: https://doi.org/10.7554/eLife.47642.020

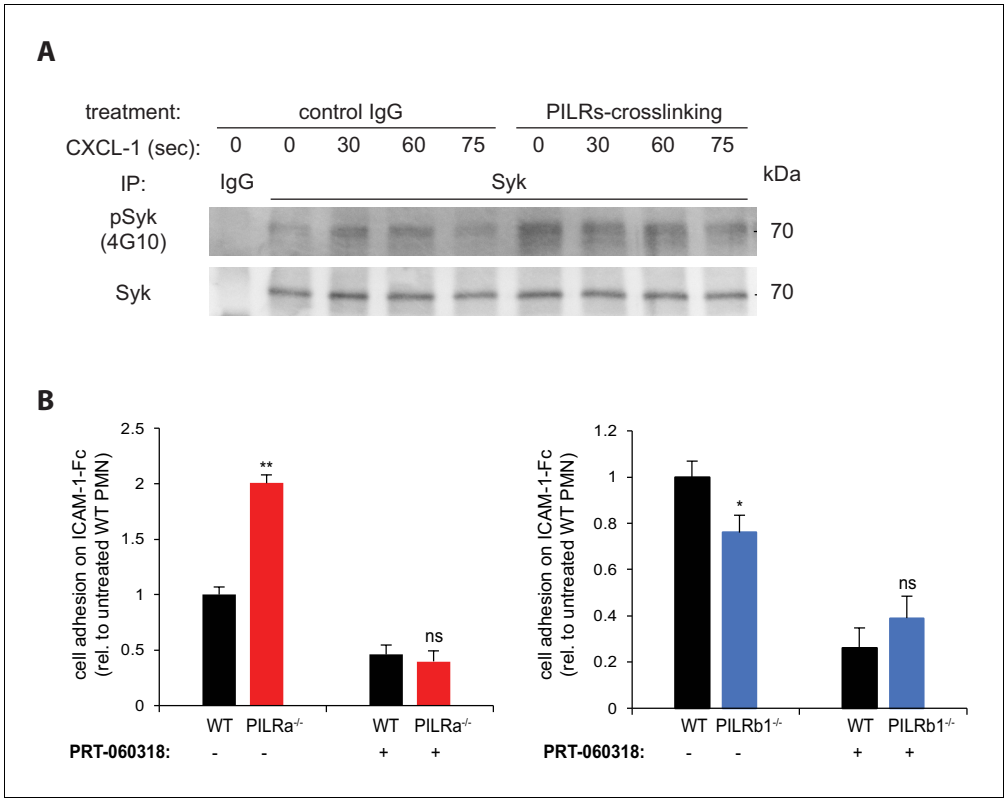

Figure 3—figure supplement 1. PILRs modulate β2 integrin activity via Syk. (**A**) PMN were pre-treated with non-crosslinking rabbit IgG or crosslinking polyclonal anti-PILRs for 15 min, and then stimulated with 100 ng/ml CXCL-1 for 0 s (unstimulated), 30 s, 60 s and 75 s, followed by fixation and cell lysis. Syk was immunoprecipitated and analyzed for phospho-Syk (4G10). (**B**) PMNs from WT (black), PILR-$\alpha^{-/-}$ (red) or PILR-$\beta1^{-/-}$ (blue) were treated with or without 1 μM Syk-inhibitor PRT-060318 for 30 min. Cells were allowed to adhere to ICAM-1-Fc coated surfaces in the presence of 100 ng/ml CXCL-1 with or without PRT-060318. Adherent cells were counted. n ≥ 12 for each genotype from at least two experiments. Error bars, SEM. Groups were compared by 2-tailed t-test. ns, not significant, *p<0.05, **p<0.01.

DOI: https://doi.org/10.7554/eLife.47642.021

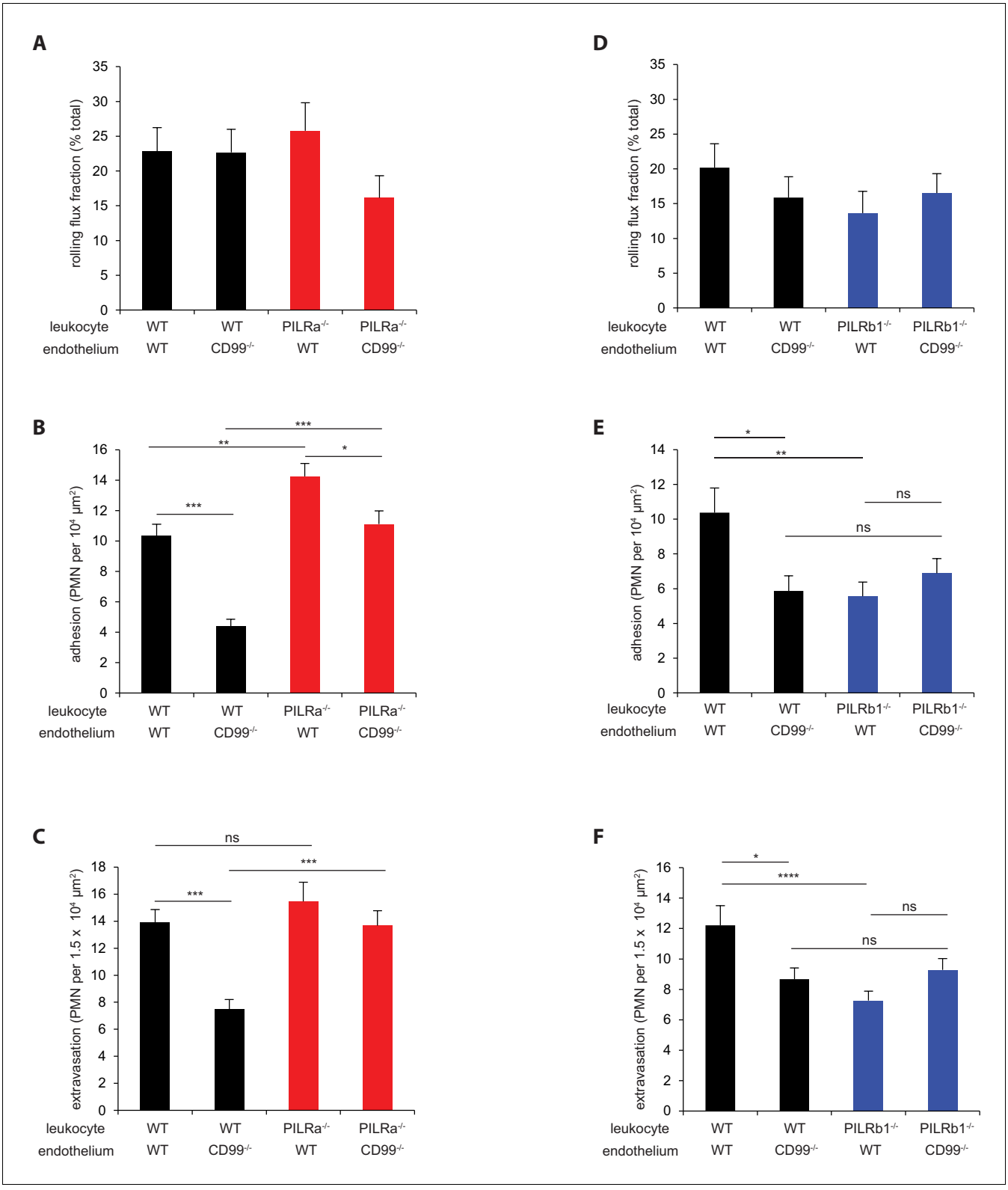

Figure 4. PILR-β1, but not PILR-α, is essential for CD99-stimulated support of neutrophil adhesion in vivo. WT or CD99$^{-/-}$ mice received bone marrow transplantation from WT (**A–F**) or PILR-α$^{-/-}$ (**A–C**) or PILR-β1$^{-/-}$ (**D–F**). IVM measurement of (**A, D**) rolling flux fraction, (**B, E**) adhesion and (**C, F**) extravasation were performed on TNF-α inflamed cremasters of the chimeric mice. Donor-Recipient: For (**A–C**), WT-WT, n = 39 vessels from five mice; WT-CD99$^{-/-}$, n = 38 vessels from five mice; PILR-α$^{-/-}$-WT, n = 39 vessels from five mice; PILR-α$^{-/-}$-CD99$^{-/-}$, n = 34 vessels from four mice. For (**D–F**), WT-WT, n = 23 vessels from four mice; WT-CD99$^{-/-}$, n = 28 vessels from five mice; PILR-β1$^{-/-}$-WT, n = 29 vessels from five mice; PILR-β1$^{-/-}$-CD99$^{-/-}$, n = 36

Figure 4 continued on next page

Figure 4 continued

vessels from five mice. Groups were analyzed by 1-way ANOVA followed by Tukey's multiple comparisons. Error bars, SEM. *p<0.05, **p<0.01, ***p<.005. Hemodynamic parameters are given in ***Tables 2*** and ***3***.

DOI: https://doi.org/10.7554/eLife.47642.031

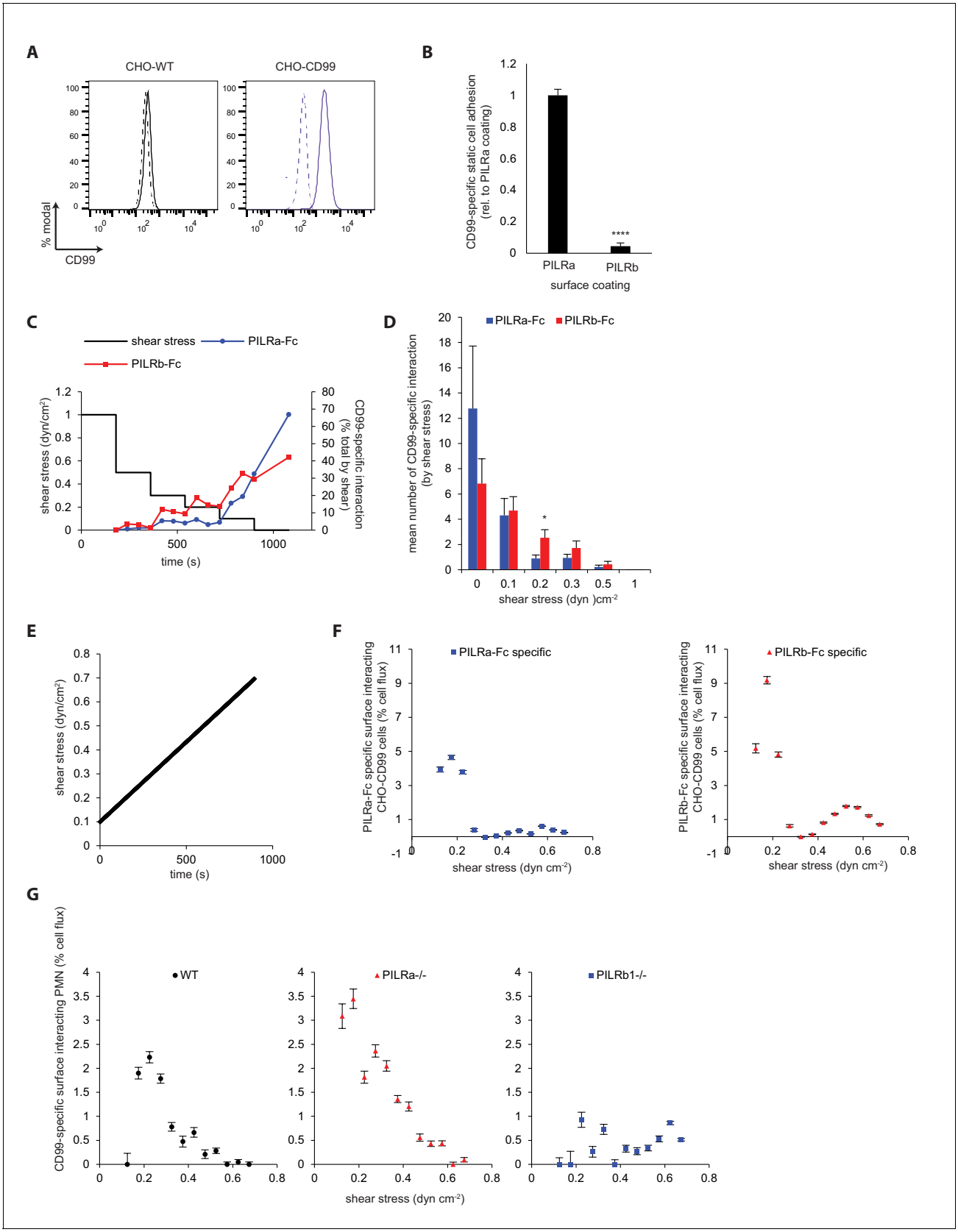

Figure 5. Shear stress enhances the interaction of CD99 with PILR-β. (**A**) CHO cells overexpressing CD99 (CHO-CD99) were constructed and analyzed for surface expression of CD99. Solid tracks, anti-CD99; dotted tracks, secondary antibody only. (**B**) 1:1 Cell mixtures of CHO and CHO-CD99 were

Figure 5 continued on next page

Figure 5 continued

allowed to adhere onto PILR-α-Fc or PILR-β-Fc coated surface at RT for 10 min (static conditions). CD99-specific cell adhesion was quantified. n = 30 fields from six experiments. (**C**) 1:1 Cell mixtures of CHO and CHO-CD99 were passed over flow chamber surfaces coated with PILR-α-Fc (blue) or PILR-β-Fc (red) at RT under stepped shear stress of 3 min interval each (black) and video recorded. CD99-specific cell-surface interactions (≥2 s) were counted every minute. (**D**) Mean number of CD99-specific interactions under the indicated shear stress (from C) were quantified. n = 8 experiments on PILR-α-Fc coating, n = 9 experiments on PILR-β-Fc coating. (**E, F**) CHO-CD99 were passed over a surface coated with PILR-α-Fc (blue), PILR-β-Fc (red) or an uncoated control surface under increasing shear stress and video recorded. Transiently interacting (≥50 ms) cells were counted and averaged from six experiments for determining fraction of PILR-specific interacting cell flux. (**G**) Experiment described as in (**E, F**) was repeated by passing WT (black), PILR-$\alpha^{-/-}$ (red) and PILR-$\beta1^{-/-}$ (blue) PMNs through CD99-Fc or control hIgG coated flow chambers. Transiently interacting (≥30 ms) neutrophils were counted and averaged from four experiments for determining the fraction of CD99-specific cell flux interactions. n = 75 measurements per 0.05 dyn/cm^2 interval for (**E–G**). Groups were compared by Mann-Whitney U-test in (**B**) and 2-tailed t-test in (**D**). Error bars, SEM. *p<0.05, ***p<.005, ****p<0.001.

DOI: https://doi.org/10.7554/eLife.47642.038

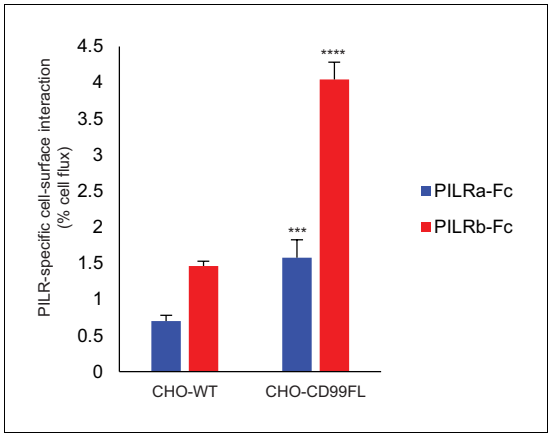

Figure 5—figure supplement 1. CD99-specific interaction with coated PILR-Fc under constant flow. Parental CHO cells (CHO-WT) or CHO cells expressing full-length CD99 (CHO-CD99FL) were passed over a surface coated with PILR-α-Fc (blue) or PILR-β-Fc (red), or over an uncoated control surface at a constant shear stress of 0.2 dyn/cm^2 at room temperature for 3 min. Videos were recorded at one frame-per-second. Transiently interacting (≥50 ms) cells were counted and averaged from three experiments per genotype per coating for determining the fraction of PILR-specific cell flux interactions. n = 180 frames per flow. Groups were compared against CHO-WT by Mann-Whitney U-test. ***p<.005, ****p<0.001.

DOI: https://doi.org/10.7554/eLife.47642.039

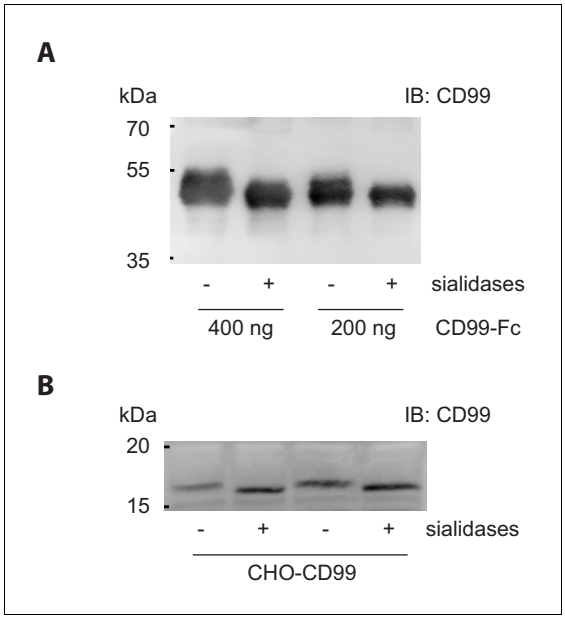

Figure 5—figure supplement 2. CD99-Fc and full-length CD99 produced in CHO cells are glycosylated. (**A**) CD99-Fc was treated with 0 or 0.3 U/ml sialidase at 37°C for 1 hr and analyzed by Western blot. (**B**) CHO-CD99 was similarly treated with sialidase. Lysate was prepared and analyzed by Western blot.
DOI: https://doi.org/10.7554/eLife.47642.041

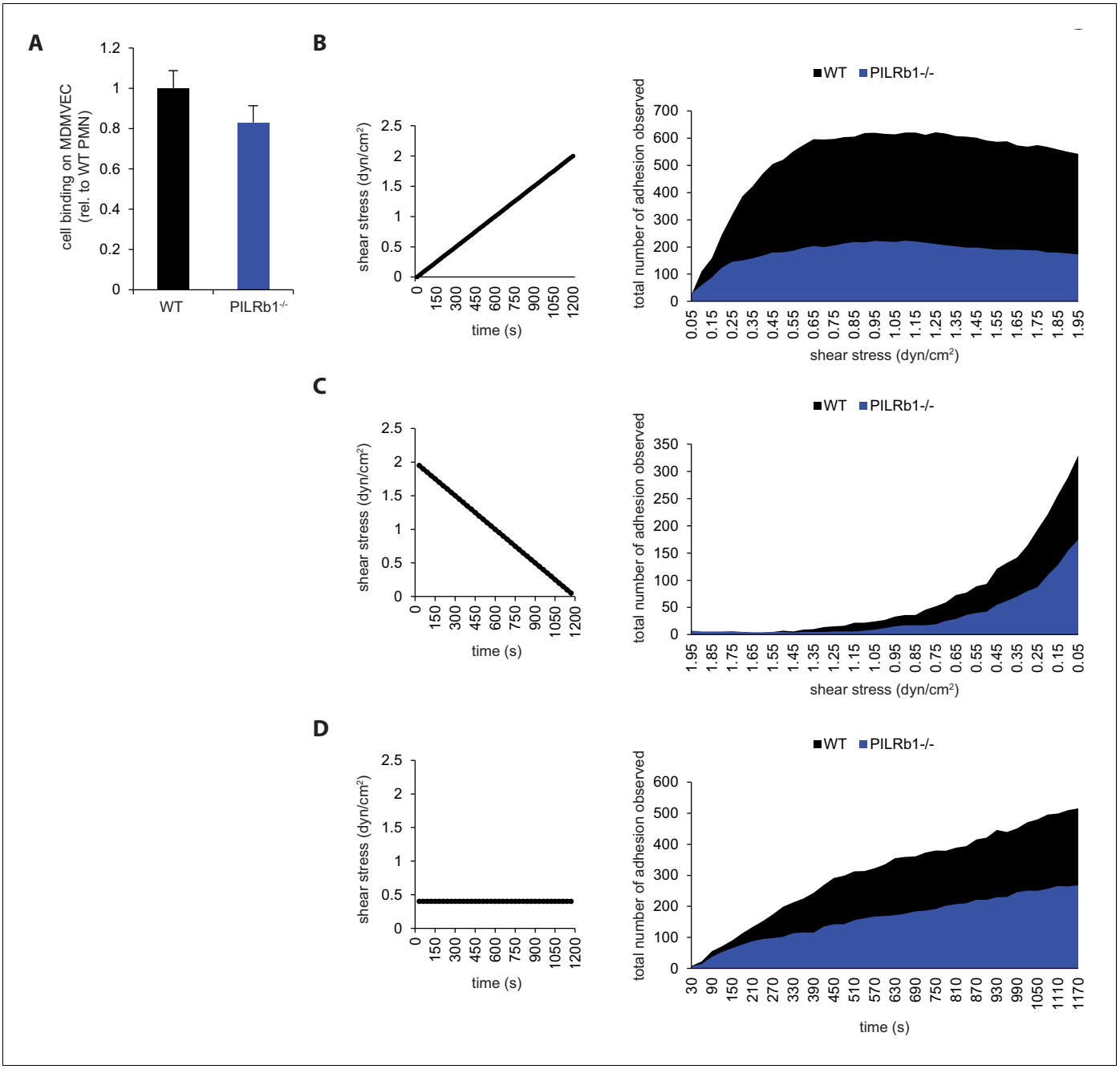

Figure 6. Shear switches on PILR-β1-stimulated adhesion of neutrophils to endothelial monolayers under flow. (**A**) PMN from WT or PILR-β1$^{-/-}$ mice were allowed to adhere onto TNF-α inflamed and CXCL-1 pretreated MDMVEC under stasis. Adherent cells were counted. n = 17 fields per genotype from two experiments. Groups were compared by 2-tailed t-test. Error bars, SEM. (**B–D**) PMN from WT or PILR-β1$^{-/-}$ mice were passed under increasing flow over TNF-α inflamed and CXCL-1 pretreated MDMVEC monolayer under an increasing shear gradient (**B**) or a shear gradient from 2 to 0 dyn/cm^2 (**C**) or a constant shear at 0.4 dyn/cm^2 (**D**) in 20 min with adhesion events (**C**) being pooled from five experiments (**B, C**) or four experiments (**D**) for each genotype under different shear stresses.

DOI: https://doi.org/10.7554/eLife.47642.047

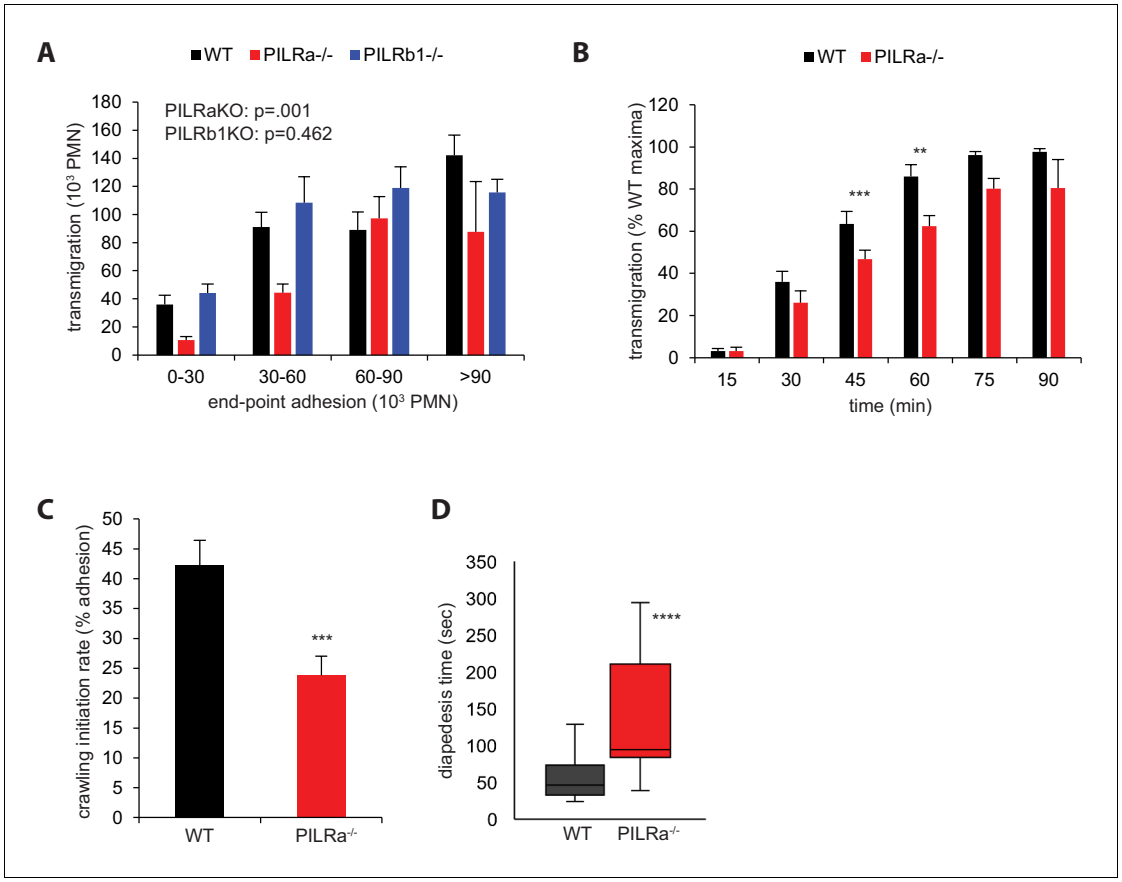

Figure 7. PILR-α supports crawling and diapedesis. (**A**) Correlation between adhesion and transmigration of WT, PILR-$\alpha^{-/-}$ and PILR-$\beta1^{-/-}$ PMNs in static transendothelial cell migration (TEM) assays through MDMVEC. n = 96 (WT), 54 (PILR-$\alpha^{-/-}$) and 41 (PILR$\beta1^{-/-}$) transwells. Knockouts were compared against WT by 2-way ANOVA followed by Holm-Sidak method for multiple comparisons. (**B**) WT and PILR-$\alpha^{-/-}$ PMN were allowed to transmigrate through MDMVEC for the indicated times. n = 4 transwells per time point per genotype from two experiments. Genotypes were compared by 2-tailed paired t-test. (**C, D**) WT and PILR-$\alpha^{-/-}$ PMNs with either genotype fluorescently labeled were mixed and passed over TNF-α inflamed MDMVEC monolayers to allow transendothelial migration at 37°C for 20 min under flow, analyzed by video recording. The fraction of crawling cells (**C**) and the time needed for diapedesis (**D**) were determined. n = 14 videos for (**C**) and n = 31 (WT) or 15 (PILR-$\alpha^{-/-}$) diapedesis events for (**D**). Groups were compared by Mann-Whitney U-test. Error bars: SEM. **p<0.01, ***p<.005, ****p<0.001.
DOI: https://doi.org/10.7554/eLife.47642.052

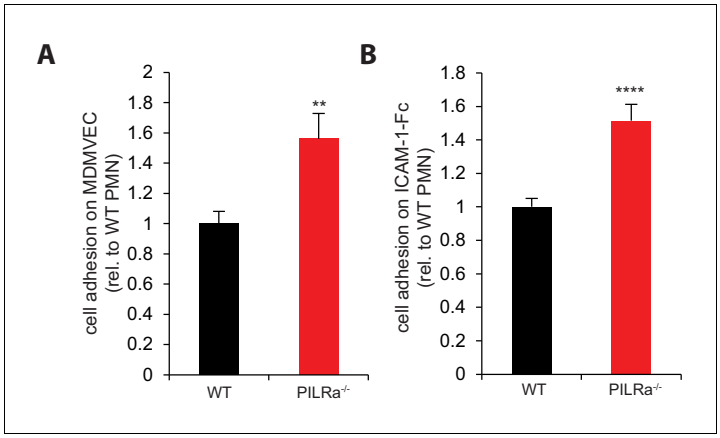

Figure 7—figure supplement 1. PILR-α suppresses adhesion on endothelial monolayers. (**A**) WT or PILR-$\alpha^{-/-}$ PMNs were allowed to adhere onto TNF-α stimulated MDMVEC and adherent cells were counted. n = 16 fields from two experiments. (**B**) WT or PILR-$\alpha^{-/-}$ PMNs were allowed to adhere on ICAM-1-Fc coated surface in the presence of 100 ng/ml CXCL-1. n = 25 fields from three experiments. Groups were compared by 2-tailed t-test. **p<0.01, ****p<0.0001.

DOI: https://doi.org/10.7554/eLife.47642.053

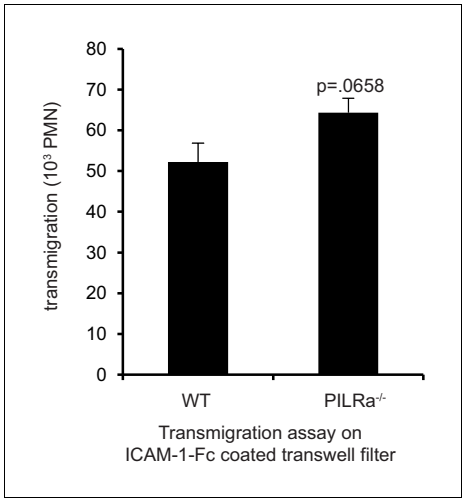

Figure 7—figure supplement 2. Effect of PILR-α on leukocyte crawling requires endothelial surface. Transmigration of WT and PILR-α- /- PMNs towards 40 ng/ml CXCL-1 through polycarbonate transwell filters (3 μm pore size) coated with 2 μg/ml ICAM-1-Fc for 1 hr at 37˚C. n = 6 transwells. Groups were compared by 2-tailed t-test.

DOI: https://doi.org/10.7554/eLife.47642.057

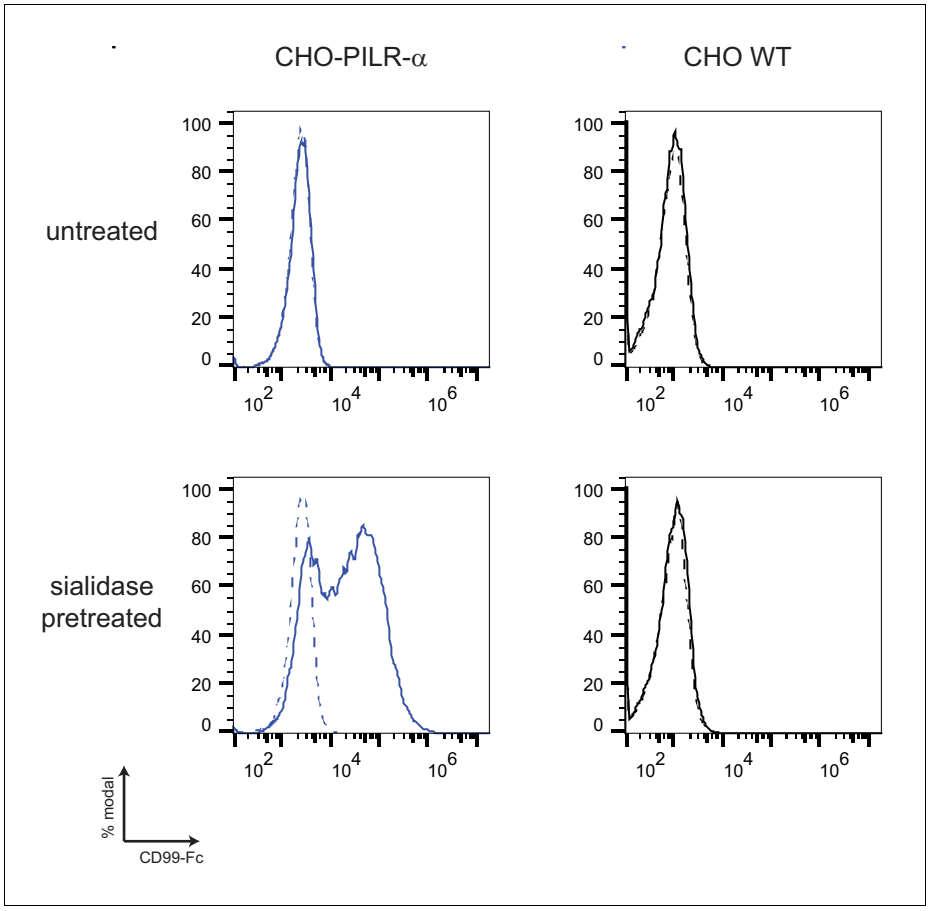

Figure 7—figure supplement 3. PILR-α on cellular surface is unavailable for CD99-Fc binding due to blockade by cis-interaction with sialylated entities. CHO- WT (black) or overexpressing PILR-α (CHO-PILR-α, blue) were treated with 0 or 0.3 U/ml sialidase at 37°C for 30 min. Cells were washed and probed for CD99-Fc binding. CD99-Fc binding on cell surface was measured by flow cytometry. Solid, CD99-Fc, dotted, control. Histograms are representative of two similar experiments.

DOI: https://doi.org/10.7554/eLife.47642.056

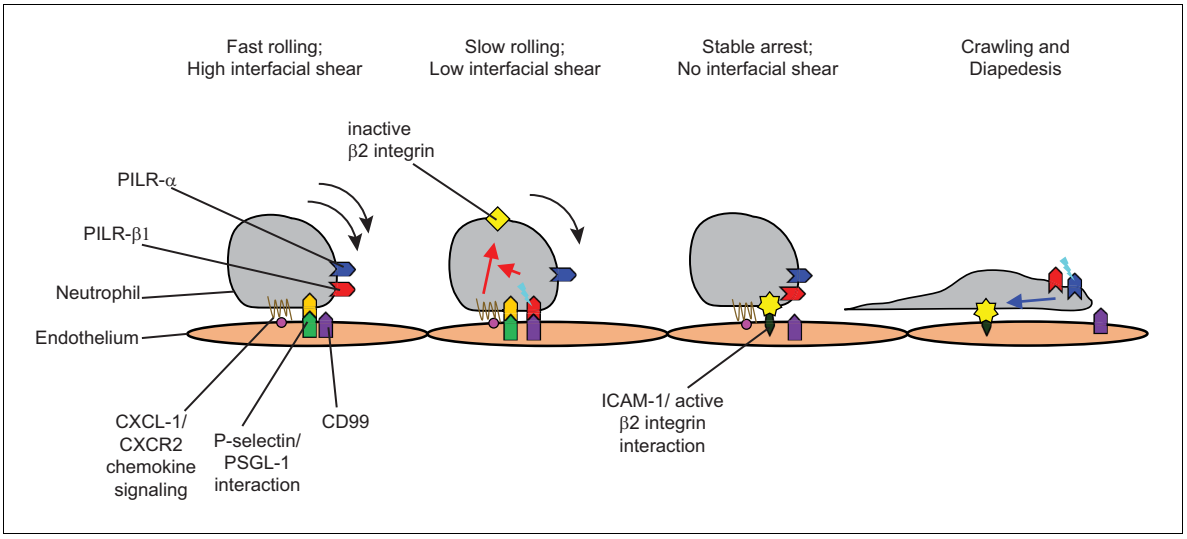

Figure 8. Graphical depiction. An antagonistic pair of receptors, PILR-β1 and PILR-α, supports neutrophil arrest and seamless transition to crawling via modulating β2 integrin activity at different steps during extravasation.

DOI: https://doi.org/10.7554/eLife.47642.062